scientific reports

Check for updates

OPEN

Oroxylin A suppressed colorectal cancer metastasis by inhibiting the activation of the TGF-β/SMAD signal pathway

Ji-Ping Cao[1,4], Yang Yan[2,4], Xin-Shuai Li[1], Long-Xun Zhu[1], Rui-Kun Hu[3]✉ & Pan-Feng Feng[1]✉

Metastatic colorectal cancer continues to have a high fatality rate, with approximately only 14% of patients surviving more than 5 years. To improve the survival rate of these patients, the development of new therapeutic drugs is a priority. In this study, we investigated the effects of Oroxylin A on the metastasis of human colorectal cancer cells and its potential molecular mechanism. This study utilised CCK8 assay, transwell assay, flow cytometry, western blot analysis, molecular docking, HE staining, immunofluorescence staining, and xenograft models. The proliferation, migration, and invasion of colon cancer cells were effectively suppressed by Oroxylin A in a dose-dependent manner. Oroxylin A has the potential to inhibit the process of epithelial–mesenchymal transition (EMT) by upregulating the expression of E-cadherin, a marker associated with epithelial cells, while downregulating the levels of N-cadherin, Snail, vimentin, and slug, which are markers associated with mesenchymal cells. In addition, 200 mg/kg of Oroxylin A inhibited the growth of colorectal tumours. Molecular docking technology revealed that Oroxylin A can bind to TGFβ and inhibit the activation of the TGFβ-smad signalling pathway. The overexpression of TGFβ weakened the inhibitory effect of Oroxylin A on the proliferation, migration, and invasion of human colorectal cancer cells, as well as the promoting effect on apoptosis. Oroxylin A inhibited the activation of the TGF-smad signalling pathway and the EMT process, thereby suppressing the migration and invasion of human colorectal cancer cells.

Keywords Colorectal cancer, Oroxylin A, Molecular docking, Metastasis, EMT, TGFβ-smad signalling pathway

Globally, colorectal cancer (CRC) is the third most common type of cancer and the second most common cause of cancer-related death[1]. A 60% increase in colon cancer mortality is expected by 2035, and a 71.5% increase in rectal cancer mortality is predicted[2]. The 5-year survival rate for metastatic colorectal cancer (mCRC) remains low (14%)[3]. Tumour metastasis plays an important role in the development of malignancy. Approximately two-thirds of cancer deaths are caused by metastases in vital organs such as the brain, lungs, and liver[4]. The prevention of tumour metastasis can delay the growth and deterioration of cancers by preventing metastatic cells from colonizing other organs[5]. Despite various therapeutic strategies being developed, the prognosis of mCRC still needs to be improved[6]. There are many reasons for treatment failure in metastatic CRC, such as adverse events caused by chemotherapy, drug nonspecificity, and drug efflux-mediated resistance resulting from the overexpression of ABC transporters, among others[7]. To improve the survival rate of these patients, the development of new therapeutic strategies is a priority[8].

There is long-standing evidence that medicinal plants have great potential for disease prevention and treatment[9]. A growing number of studies have investigated the effects of traditional Chinese medicine (TCM) on tumour treatment and have shown the importance of TCM in recent years. However, TCM has a unique, novel pharmacological mechanism and advantages, including limited toxic side effects and the same curative effect as conventional therapies[10,11]. Oroxylin A, which is extracted from Scutellaria baicalensis Georgi (a traditional Chinese medicinal plant), has been proven to have broad functions, such as anticancer, anti-inflammatory, neuroprotective, and anticoagulation effects[12–14]. In particular, Oroxylin A has attracted considerable attention for

[1]Department of Pharmacy, Afliated Hospital 2 of Nantong University, No. 666, Shengli Road, Nantong 226001, China. [2]The Ninth Geological Brigade of Jiangxi Geological Bureau, Nanchang, China. [3]Personnel Department, Affiliated Maternity and Child Health Care Hospital of Nantong University, No.399, Shiji Road, Nantong 226001, China. [4]These authors contributed equally: Ji-Ping Cao and Yang Yan. ✉email: huruikun2021@163.com; 929083891@qq.com

its antitumour properties. Cao et al. demonstrated that Oroxylin A could remodel the stromal microenvironment and inhibit breast cancer metastasis[15]. Wei et al. demonstrated that the effect of Oroxylin A on snail-expressing non-small-cell lung cancer cells is mediated via the suppression of the ERK/GSK-3β signalling pathway[16]. Huo et al. demonstrated that Oroxylin A exhibited notable antimetastatic effects on HCC cells both in vitro and in vivo. This antimetastatic effect is due to an Oroxylin A-induced increase in NAG-1 expression levels[17]. However, the mechanism of action of Oroxylin A in colorectal cancer metastasis is not fully known, and there is an urgent need to clarify the mechanism involved.

In this study, in vivo experiments (xenograft tumour models) and in vitro experiments (cell biology experiments) were used to study the effects of Oroxylin A on colorectal cancer metastasis to provide information to aid in clinical treatment.

Materials and methods

Reagents and antibodies

Oroxylin A (CAS:480-11-5) and SRI-011381 hydrochloride (CAS:2070014-88-7) were purchased from MedChemExpress. Anti-E-cadherin (ab231303), anti-N-cadherin (ab98952), anti-TGFβ (ab215715), anti-Smad2 (ab40855) and anti-Smad3 (ab40854) antibodies were purchased from Abcam (Cambridge, Britain). Anti-Snail (A5243) and anti-Vimentin (A11952) were purchased from ABclonal (Wuhan, China). Anti-slug (PA5-73015) was purchased from Thermo Fisher Scientific. Goat anti-mouse and goat anti-rabbit secondary antibodies were purchased from LI-COR (Lincoln, USA).

Cell culture

Colorectal cell lines (HCT116, SW620, and DLD-1) and human colon cells (NCM460) were purchased from the National Collection of Authenticated Cell Cultures and Shanghai Yaji Biotechnology, respectively. The cells were cultured in DMEM (NCM460 and HCT116), L-15 medium (SW620), or RPMI-1640 medium (DLD-1) supplemented with 10% foetal bovine serum and 1% penicillin–streptomycin at 37 °C in an atmosphere of humidified 5% carbon dioxide.

CCK-8 assay

The proliferation of colorectal cell lines (HCT116, SW620, and DLD-1) in vitro was assessed using a CCK-8 assay. In brief, the cells were plated in 96-well plates at a density of 50,000 cells/well overnight to adhere before being treated with Oroxylin A 0, 10, 20, or 40 μM for 48 h. CCK-8 solution (10 μL) was added to each well and incubated at 37 °C for 4 h in a humidified atmosphere containing 5% CO_2. A microplate reader was used to determine the absorbance of each well at 450 nm (450 nm OD value). Cell viability was calculated using the following formula: $(OD_{drug} - OD_{blank})/(OD_{control} - OD_{blank}) \times 100\%$.

Transwell assay

The cells that were treated with Oroxylin A (0, 10, 20, or 40 μM) were cultured for 48 h and then plated in the upper chamber with or without Matrigel precoating for the migration or invasion assays. The lower chamber contained DMEM (500 μL) supplemented with 10% FBS. After incubation for 24 h, the migrated and invaded cells were fixed in 4% paraformaldehyde for 30 min at room temperature and stained with 0.5% crystal violet for another 20 min. Light microscopy was used to count the number of cells in at least six randomized fields.

Flow cytometry

Following the manufacturer's instructions, an Annexin V-FITC/Propidium Iodide (PI) Apoptosis Detection Kit (Thermo Fisher Scientific, E-CK-A211) was used to measure cell (HCT116, SW620 and DLD-1) apoptosis. Human colorectal cells were digested, plated in a 6-well plate, treated with Oroxylin A (0, 10, 20, and 40 μM), and continuously cultured for 48 h at 37 °C in a CO_2 incubator. The cells were then detached in the logarithmic phase with trypsin, resuspended in PBS, washed twice, centrifuged at 300 × g for 5 min, and the supernatant was discarded. As part of the centrifugation process, the supernatant was discarded after the cells were washed in prechilled PBS. Then, the cells were collected and resuspended in 100 μL of 1× Annexin V binding buffer. A total of 2.5 μL of PI reagent and 2.5 μL of Annexin V-FITC were incubated with the cells for 15–20 min in the dark at room temperature. Finally, 400 μL of 1 × Annexin V binding buffer was added to the EVs and flow cytometry analysis was conducted immediately thereafter.

Western blot analysis

Western blot analysis was performed to determine the protein expression levels of E-cadherin, N-cadherin, vimentin, snail, slug, TGFβ, smad2, and smad3. Protein was extracted using a total protein extraction kit from Keygen Biotech (Nanjing, China) and quantified using a BCA protein assay kit. An electrophoresis of 10% SDS–PAGE was performed to separate the total protein. After being transferred to NC membranes, they were blocked with 5% nonfat milk for 2 h at room temperature, followed by incubation with the primary antibody overnight at 4 °C. The samples were then incubated for 1 h at 37 °C with a secondary antibody. ImageJ software was used to analyse the grayscale values of the Western blot protein bands.

Immunofluorescence staining

Human colorectal cells were then treated with different concentrations of Oroxylin A (0, 10, 20, and 40 μM) and cultured for 24 h. After being fixed with 4% paraformaldehyde (PFA) for 20 min at room temperature, the cells were rinsed three times with PBS, permeabilized with 0.1% Triton-X 100 for 10 min, and then rinsed three times with PBS for 5 min each. The cells were subsequently incubated overnight at 4 °C with primary antibodies (anti-E-cadherin, anti-N-cadherin, and anti-TGFβ) after being blocked for 60 min with 3% BSA. The cells were treated

with a secondary antibody for 1 h and then with DAPI for 5 min at room temperature. Finally, we examined and photographed the samples under a fluorescence microscope and analysed the fluorescence intensity using Image-Pro Plus 6.0 software.

Molecular docking

To analyse the binding affinities and modes of interaction between the drug and its targets, AutodockVina 1.2.2, an in silico protein–ligand docking software, was used. The molecular structure of Oroxylin A was retrieved from PubChem Compound (https://pubchem.ncbi.nlm.nih.gov/). The 3D coordinates of TGFβ were downloaded from the PDB (http://www.rcsb.org/pdb/home/home.do). For docking analysis, all protein and molecular files were converted into PDBQT format with all water molecules excluded, and polar hydrogen atoms were added. The grid box was centred to cover the domain of each protein and to accommodate free molecular movement. Molecular docking studies were performed via AutoDock Vina 1.2.2 (http://autodock.scripps.edu/).

Xenograft tumour models

Standard conditions were used to house female BALB/c nude mice (4 weeks old) for 1 week, which were purchased from Beijing HFK Bio-Technology Co., Ltd. Fifteen mice were used in this study. All animal experiments were approved by the Ethics Committee for Animal Experiments of Nantong University (S20220221-015). Approximately 1×10^6 viable HCT116 cells were resuspended in PBS (100 μL) and injected subcutaneously into BALB/c nude mice. The health of the mice was monitored, and tumour sizes were measured every 2 days. As soon as the tumour volume reached approximately 50 mm^3, the mice were ready for dosing experiments. The mice were divided into three groups of five in each group (control, Oroxylin A 100 mg/kg, and Oroxylin A 200 mg/kg). Every three days after Oroxylin A was administered, the tumour volume and body weight were measured. The mice were then sacrificed via an intraperitoneal injection of ketamine (100 mg/kg) prepared with a physiological saline solution by cervical dislocation, and the tumours were harvested after 20 days of Oroxylin A treatment. Finally, the tumours were photographed, weighed, and sectioned for immunohistochemistry and haematoxylin and eosin (HE) staining. During the entire duration (30 days) of this study, no mice were found to be in poor health or died. Studies involving animals were performed in accordance with the recommendations in the ARRIVE guidelines.

10 RT–PCR

The extraction of total RNA was performed using TRIzol reagent, followed by reverse transcription into cDNA via a ReverTra Ace qPCR RT kit (manufactured by Toyobo Co., Ltd., Japan). Real-time PCR (RT-PCR) was performed on a 7500 Fast Real-Time PCR System (manufactured by Applied Biosystems, USA) with SYBR Green Real-time PCR Master Mix (manufactured by Toyobo Co., Ltd., Japan) following the recommended reaction system provided by the manufacturer. The RT-PCR protocol consisted of an initial annealing step at 95 °C for 3 min, followed by amplification for 40 cycles at 95 °C for 10 s and 60 °C for 30 s. The results are presented as the relative gene quantity (RQ) calculated using the formula $RQ = 2^{-\Delta\Delta Ct}$.

Statistical analysis

All methods were performed in accordance with relevant guidelines and regulations. All methods were reported in accordance with ARRIVE guidelines. The data are expressed as the means ± SDs of at least three independent experiments unless otherwise specified. An analysis of variance was conducted using a one-way ANOVA, followed by a Student's t test. Differences between the control group and the experimental group were considered statistically significant when the p value was less than 0.05. All the data and figures were generated via GraphPad Prism 5.0 and Photoshop CS5.1.

Results

Effects of Oroxylin A on HCT116, DLD-1 and SW620 cell proliferation

The structure of Oroxylin A is shown in Fig. 1A. NCM460 was used as a control cell line (NC) for normal human colorectal epithelial cells. As shown in Fig. 1B, the proliferation and viability of human colorectal epithelial cells were not affected by Oroxylin A. However, Oroxylin A significantly inhibited the growth of CRC cells in a dose-dependent manner, as shown in Fig. 1C–E. These results indicate that Oroxylin A is not cytotoxic to normal cells but exerts cancer cell growth inhibitory effects.

Oroxylin A induces the apoptosis of HCT116, DLD-1, and SW620 cells

Flow cytometry was used to investigate whether Oroxylin A affects the apoptosis of human colorectal cells after treatment with Oroxylin A (0, 10, 20, or 40 μM) for 24 h. As shown in Fig. 2A-C, Oroxylin A significantly induced the apoptosis of HCT116, DLD-1, and SW620 cells. Furthermore, an increase in the percentage of apoptotic cells was correlated with an increase in Oroxylin A concentration. The percentage of apoptotic HCT116 cells increased from 1.1 to 50.80%, that of DLD-1 cells increased from 1.09 to 53.2%, and that of SW620 cells increased from 1.42 to 30.9%. Thus, these results suggest that Oroxylin A can induce cell apoptosis in human colorectal cancer cells after 24 h of treatment.

Oroxylin A suppresses HCT116, DLD-1 and SW620 cell metastasis and invasion

To analyse the effects of Oroxylin A on human colorectal cancer cell migration and invasion, transwell assays were performed. Compared with the control group, Oroxylin A significantly inhibited migration after treatment with different concentrations (Fig. 3A–C). Similarly, following treatment with 10, 20, or 40 μM oOroxylin A for 24 h, the number of invading cells was significantly lower than that in the control group (Fig. 4A–C). These results demonstrate that Oroxylin A inhibits the migration and invasion of human colorectal cancer cells in vitro.

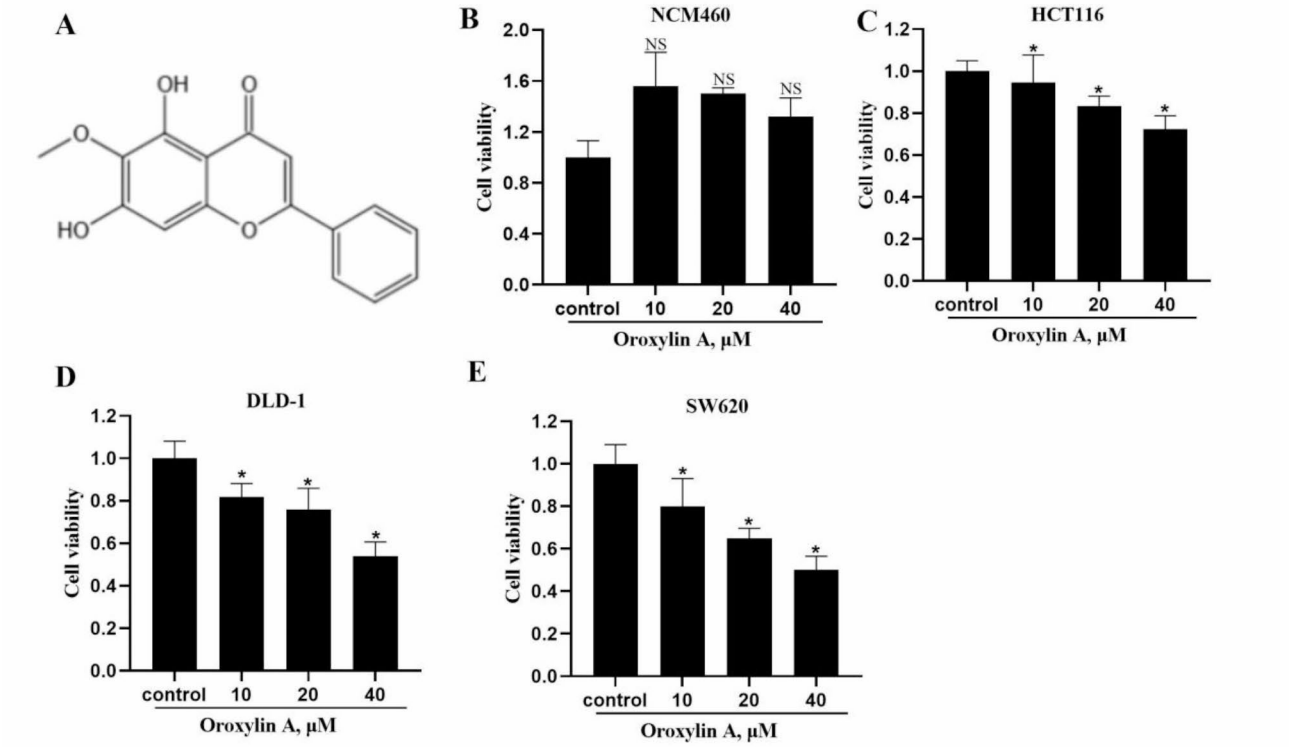

Fig. 1. Effects of Oroxylin A on HCT116, DLD-1 and SW620 cell proliferation. (**A**) Structure of Oroxylin A. (**B**–**E**) CCK-8 assessment of the impact of Oroxylin A on the viability of normal human colorectal epithelial cells (NCM460) and human colorectal cancer cells (HCT116, SW620, DLD-1). "*" indicates a difference compared with the control group ($P < 0.05$), $n = 5$.

Oroxylin A inhibits tumour growth in HCT116 xenografts in vivo

To verify the inhibitory effects of Oroxylin A on colorectal cancer growth in vivo, the HCT116 cell xenograft model was developed. The results suggested that Oroxylin A (200 mg/kg) treatment significantly reduced the tumor volume and weight compared to controls (Fig. 5A–C). However, there was no significant difference in tumor size and volume after treatment with Oroxylin A (100 mg/kg). In this study, immunohistochemical staining was used to monitor Ki67 expression. We found that Ki-67 protein expression was decreased by Oroxylin A (200 mg/kg) in HCT116 tumor tissue (Fig. 5D,E). In addition, Oroxylin A increased the mRNA level of the pro-apoptotic gene Bax and cleaved caspase-3 (Fig. 5F).HE staining of the tumor showed that in the control group, the shape of the tumor was full, the tumor cells were evenly distributed and grew disordered, while in the high-dose group (200 mg/kg), a large area of dead tissue and vacuoles were found in the center of the tumor (Fig. 5G). In addition, after treatment with Oroxylin A (200 mg/kg), HE staining of the liver and intestine showed no evidence of normal tissue toxicities (Fig. 5H,I). Meanwhile, we examined the effects of Oroxylin A on EMT and the TGFβ signaling pathway-related gene expression, and the results showed that Oroxylin A inhibited the EMT process and the TGFβ signaling pathway (Fig. 5J,K). The subsequent cell experiments continued to verify this conclusion.

Oroxylin A inhibits metastasis via the inhibition of the EMT process

To assess whether Oroxylin A suppresses EMT-mediated CRC metastasis, we evaluated the EMT index in human colorectal cancer cells exposed to Oroxylin A (0, 10, 20, or 40 μM). A significant increase in E-cadherin expression was observed in human colorectal cancer cells after treatment with different concentrations of Oroxylin A, but a decrease in N-cadherin, vimentin, snail and slug expression was observed (Fig. 6A,B,E–G). In addition, the immunofluorescence results also revealed a decrease in N-cadherin expression and an increase in E-cadherin expression in the group treated with Oroxylin A (Fig. 6C,D). These findings indicate that Oroxylin A suppresses the metastasis of human colorectal cancer cells by inhibiting EMT.

Target prediction underlying Oroxylin a inhibition of EMT via the molecular docking method

Next, we explored the molecular mechanism by which Oroxylin A suppresses EMT in human colorectal cancer cells. TGF-β is widely considered an EMT inducer that can induce cell polarity loss, reduce cell adhesion and increase migration. Therefore, we hypothesized that the migration of human colorectal cancer cells could be inhibited by the inhibition of EMT through the TGF-β signalling pathway. To further investigate this hypothesis,

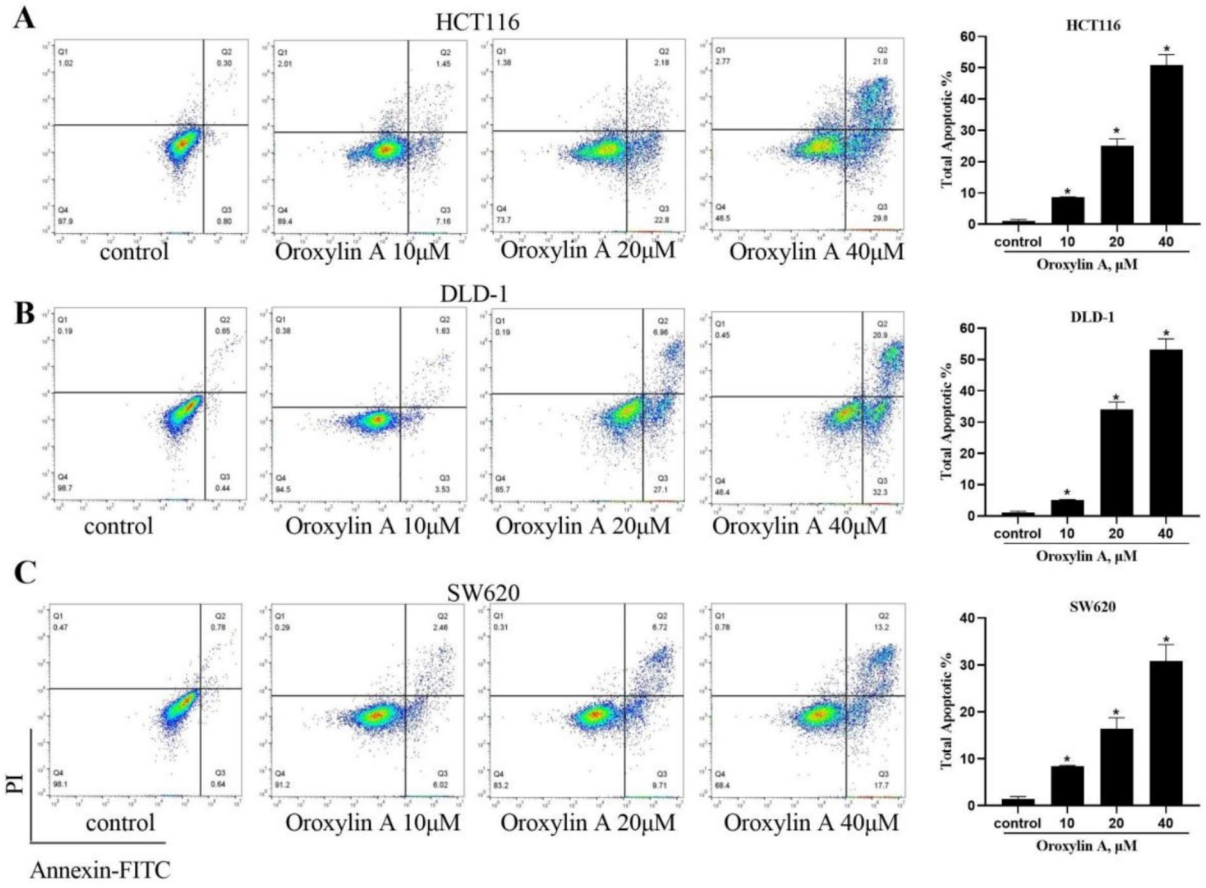

Fig. 2. Oroxylin A effectively induces apoptosis in human colon cancer cells in a dose-dependent manner. The apoptotic levels of HCT116, DLD-1, and SW620 cells were measured and analysed via flow cytometry. The symbol "*" denotes statistical significance compared to the control group ($P < 0.05$), with a sample size of $n = 3$.

molecular docking techniques were used to analyse the interactions between Oroxylin A and the TGF-β receptor. Figure 7A shows the 3D structure of Oroxylin A. The interaction diagrams between Oroxylin A and TGFβRs (TGFβR1 and TGFβR2) are shown in Fig. 7B-C. Oroxylin A forms two conventional hydrogen bonds with HIS283 and ASP351 of TGFβR1, and one conventional hydrogen bond with HIS328 of TGFβR2. The results demonstrated that Oroxylin A can interact with TGFβ. RT-PCR, Western blot and immunofluorescence assays revealed that the expression of TGFβ was inhibited by Oroxylin A in a dose-dependent manner (Fig. 7D-G). The activation of Smad signalling is crucial for mediating TGFβ-induced EMT[18]. Therefore, we further investigated the effect of Oroxylin A on the activation of the Smad signalling pathway stimulated by TGF-β. We found that Oroxylin A inhibited the activation of the Smad signalling pathway, which manifested as a decrease in the phosphorylation of Smad2 and Smad3 (Fig. 7H,I). These results support that Oroxylin A may affect the migration of human colorectal cancer cells via the TGFβ-Smad signalling pathway.

TGFβ overexpression attenuates the effect of Oroxylin A on human colorectal cancer cells

To further confirm that the TGFβ-Smad signalling pathway is involved in the inhibitory effect of Oroxylin A on the migration of human colorectal cancer cells, we selected SRI-011381 hydrochloride, which is an agonist of the transforming growth factor-β (TGF-β) pathway[19], to overexpress TGFβ. We found that coculture of Oroxylin A with SRI-011381 hydrochloride increased the expression of TGFβ, phosphorylated smad2, and smad3 (Fig. 8A–C). In addition, the overexpression of TGFβ weakened the inhibitory effect of Oroxylin A on the proliferation, migration, and invasion of human colorectal cancer cells, as well as the promoting effect on apoptosis (Fig. 8D–G). These results support that Oroxylin A inhibited colorectal cancer through the TGFβ-smad signalling pathway.

Discussion

Colorectal cancer is the third most common malignant tumour, among which the cases in China account for up to 31% of all cases globally, and its incidence and mortality are still increasing[20]. Due to its insidious onset, patients are commonly diagnosed with advanced-stage disease, and treatment consists of surgery combined with radiotherapy[21]. Natural products have been used to treat many malignant diseases, and an increasing number

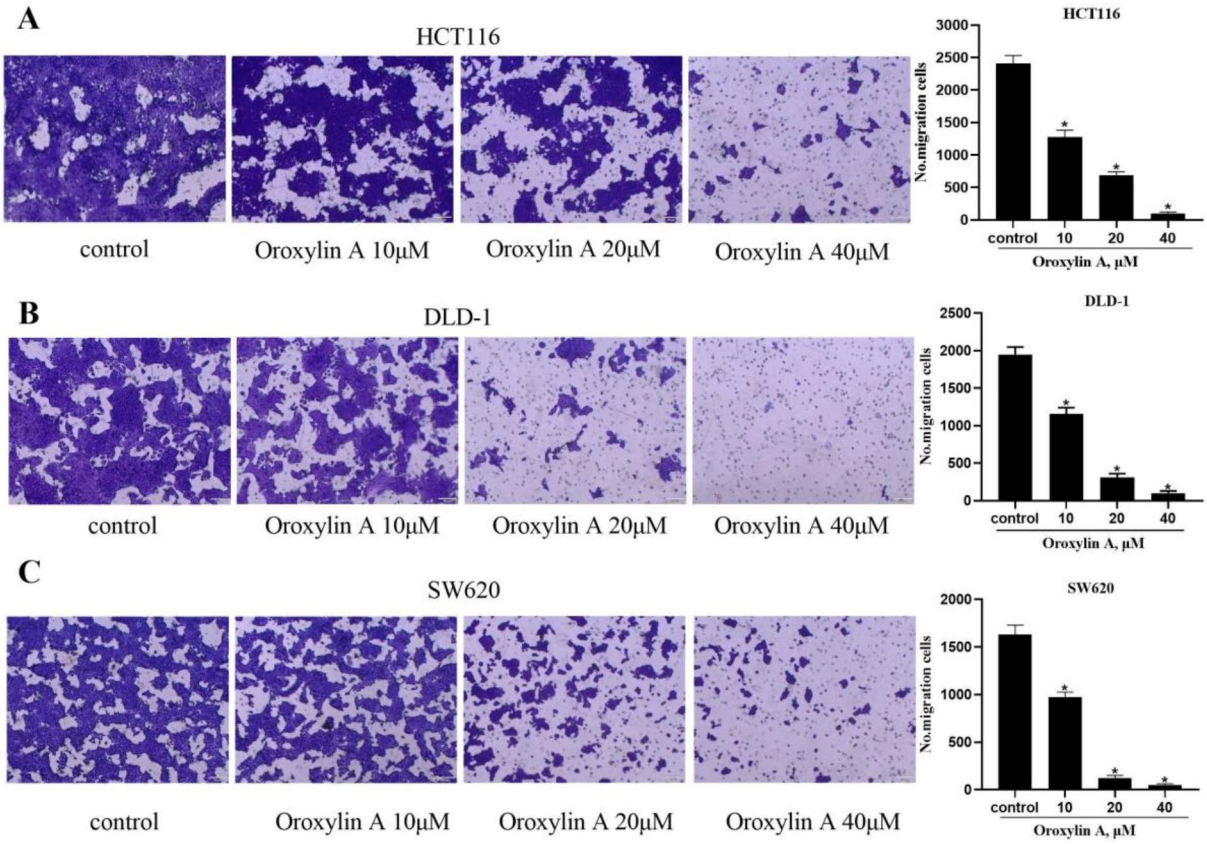

Fig. 3. Oroxylin A significantly inhibits of metastasis of human colorectal cancer cells. The migratory potential of HCT116, DLD-1 and SW620 cells was assessed via a transwell assay. The symbol "*" denotes a statistically significant difference compared with the control group ($P < 0.05$), with a sample size of $n = 3$.

of studies have shown that natural medicines play important roles in the treatment of these diseases, especially in the treatment of cancer. Oroxylin A, which is a flavonoid derivative with strong biological activity, has shown remarkable efficacy in preclinical studies[22]. In this study, in vitro experiments confirmed that Oroxylin A can inhibit the proliferation (Fig. 1) and promote the apoptosis (Fig. 2) of colorectal cancer cells. Moreover, in vivo experiments revealed that Oroxylin A inhibited tumour growth (Fig. 5A–E), which was consistent with the results of the in vitro experiments. In addition, there was no obvious toxicity to the liver or intestines (Fig. 5G,H).

Malignant tumour metastasis remains a leading cause of mortality among cancer patients globally[23]. Consequently, addressing cancer metastasis is of paramount importance in clinical interventions. Epithelial–mesenchymal transition (EMT) is a developmental process that facilitates the acquisition of invasive and metastatic characteristics by carcinoma cells[24,25]. During the process of epithelial–mesenchymal transition (EMT), the expression of E-cadherin, an adhesion molecule responsible for maintaining intercellular adhesion and tight arrangement, is reduced. Moreover, there is an increase in the expression of vimentin, a molecular marker associated with mesenchymal characteristics. This alteration leads to weakening of the junction between epithelial cells and subsequently results in loss of cellular polarity. In this study, we found that Oroxylin A increased the expression of E-cadherin (Fig. 6A,C) and decreased the expression of N-cadherin (Fig. 6B,D), indicating that Oroxylin A inhibited the metastasis and invasion of colorectal cancer by inhibiting the process of EMT.

Diverse signalling pathways may participate in the process of EMT. Overproduction of TGFβ is observed in almost all advanced human tumours, and it is directly associated with the advancement of tumour growth, invasion, and metastasis[26]. TGF-β can be acquired by tumours from various sources, such as the cancer cells themselves and the neighbouring tumour stroma[27]. TGF-β plays a significant role in promoting tumour progression at advanced stages, facilitating the onset of EMT. To confirm that TGFβ is involved in the EMT inhibition process caused by Oroxylin A, we used a molecular docking technique. The interaction between Oroxylin A and TGFβ was confirmed through the formation of two conventional hydrogen bonds with HIS283 and ASP351 of TGFβR1 (Fig. 7B), as well as one conventional hydrogen bond with HIS328 of TGFβR2 (Fig. 7C). These findings suggest that Oroxylin A has the potential to interact with TGFβ in conventional hydrogen bonds. The protein expression of TGFβ was significantly decreased in a dose-dependent manner (Fig. 7D,E). In terms of mechanism, the induction of EMT by TGF-β occurs through the phosphorylation of Smad2 and Smad3[28]. The

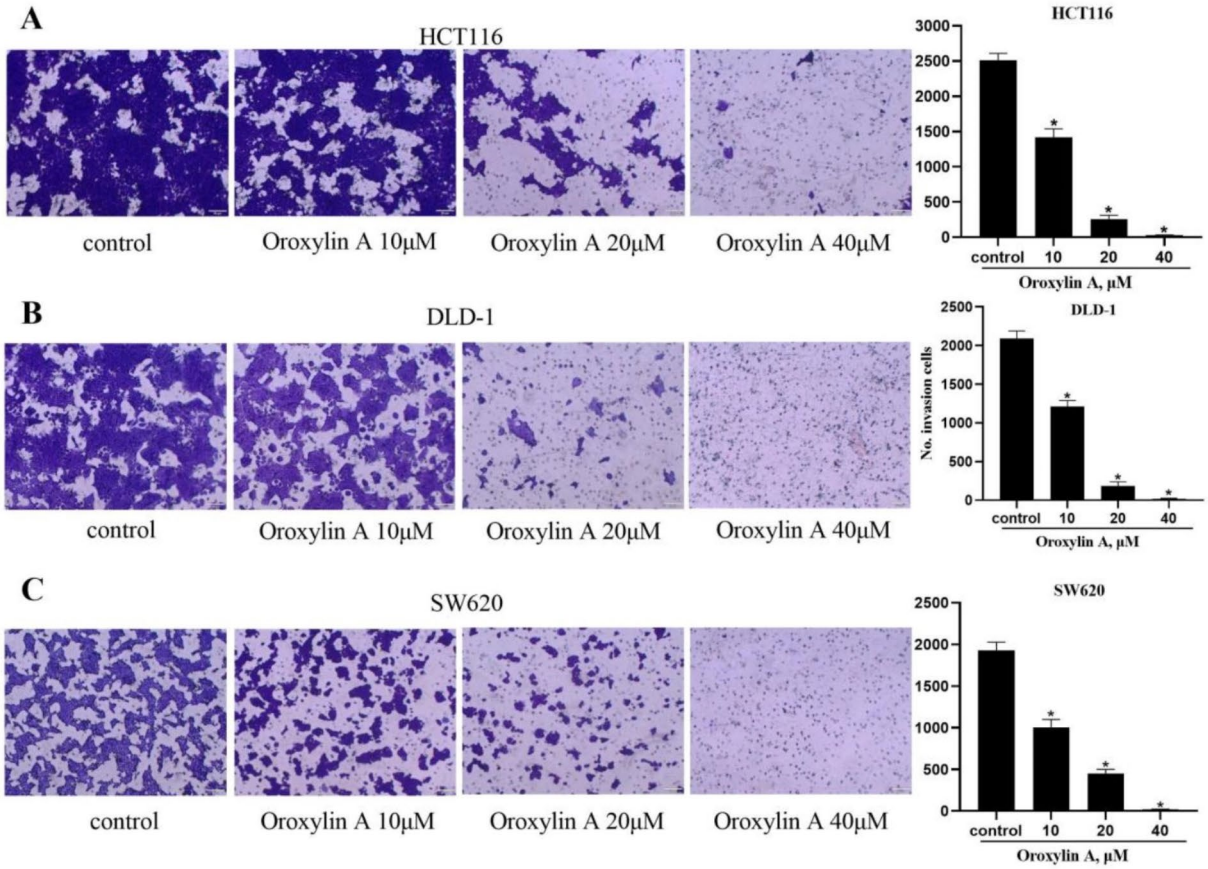

Fig. 4. Oroxylin A significantly inhibits invasion of human colorectal cancer cells. The invasive potential of HCT116, DLD-1 and SW620 cells was assessed by transwell assays. The symbol "*" denotes a statistically significant difference compared with the control group ($P < 0.05$), with a sample size of $n = 3$.

expression of transcriptional repressors such as vimentin, snail, and slug is subsequently induced by activated Smads[18]. We found that the expression of phosphorylated smad2 and smad3 was reduced (Fig. 7G,H).

To further confirm that the migration and invasion of colorectal cancer cells are inhibited by Oroxylin A through the TGF-β-smad signalling pathway, we used SRI-011381 hydrochloride to overexpress TGF-β. Compared with that in the Oroxylin A group, the expression of TGF-β in the Oroxylin A and SRI-011381 hydrochloride coculture groups was greater, and the expression of phosphorylated smad2 and smad3 was greater (Fig. 8A–C). In the cell experiments, the combination of Oroxylin A and SRI-011381 hydrochloride weakened the inhibitory effect of Oroxylin A on the proliferation, migration, and invasion of colorectal cancer cells and weakened the ability of Oroxylin A to promote apoptosis (Fig. 8D–G). Taken together, these results suggest that Oroxylin A inhibits the EMT process through the TGF-β-smad signalling pathway and subsequently inhibits the migration and invasion of human colorectal cancer cells as summarized in Fig. 9 which was drawn by Figdraw.

Conclusions

In vitro experiments revealed that Oroxylin A inhibited the proliferation, migration, and invasion and promoted the apoptosis of colorectal cancer cells. In vivo experiments also revealed that Oroxylin A reduced tumour size and volume without causing obvious toxicity to the liver or intestine. Molecular mechanism studies revealed that Oroxylin A inhibited the activation of the TGF-smad signalling pathway and the EMT process, thereby suppressing the migration and invasion of human colorectal cancer cells.

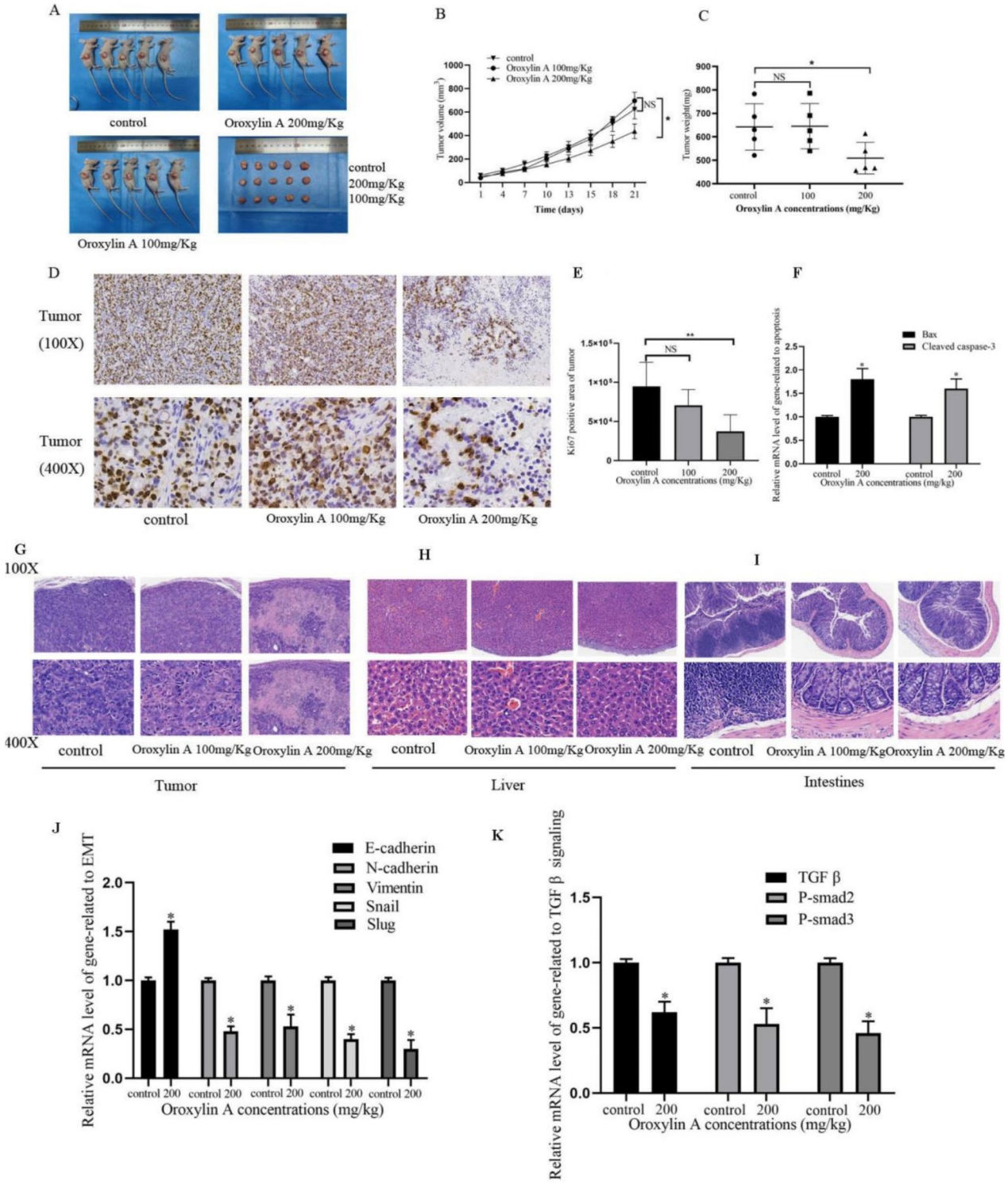

Fig. 5. The inhibitory efects of Oroxylin A on the development and growth of xenograft colorectal tumors in vivo. (**A**) Representative images of tumors in mice treated with Oroxylin A (100 mg/kg and 200 mg/kg). (**B**,**C**) Tumor volume and tumor weight was reduced in Oroxylin A-treated mice. (**D**,**E**) Ki-67 IHC staining of xenograft tumors. Original magnifcation 400×. Scale bar = 50 μm. H-scores of the Ki67 staining. (**F**) RT-PCR experiments showed that Oroxylin A increased the mRNA level of the pro-apoptotic gene Bax and cleaved caspase-3. (**G**–**I**) Representative images of tumor, liver and intestines with H&E staining, Scale bars = 50 μm. (**J**) RT-PCR experiments showed that Oroxylin A inhibited the EMT process and TGFβ signaling by regulating the expression ofgenes related to EMT and TGFβ signaling. $n = 5$. "*" $p < 0.05$, "**" $p < 0.01$ vs. the control group.

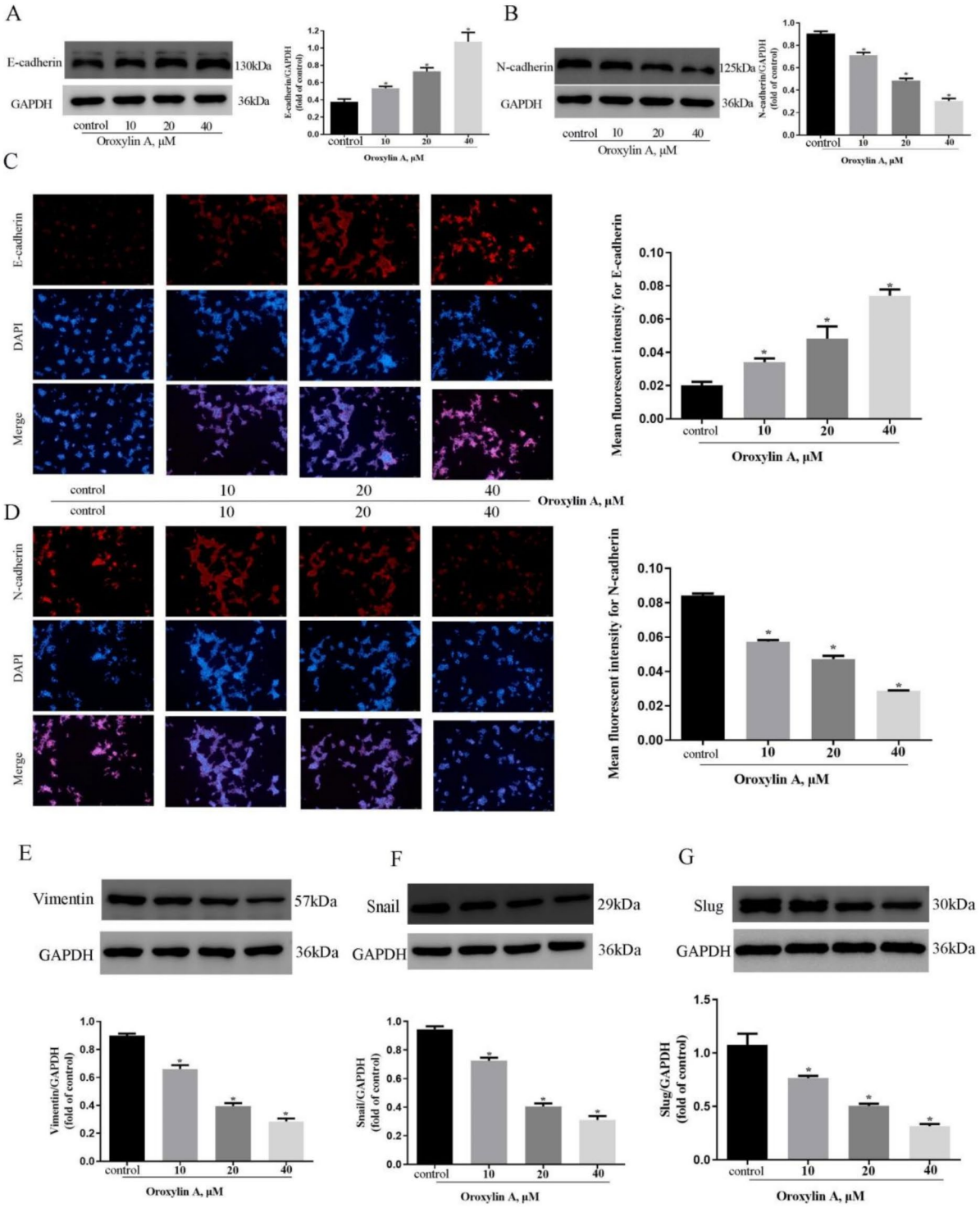

Fig. 6. Oroxylin A effectively suppresses the process of epithelial–mesenchymal transition (EMT). (**A**–**D**) Western blot analysis revealed a significant increase in E-cadherin expression and a decrease in N-cadherin expression in Oroxylin A-treated HCT116 cells compared with those in the control group. Immunofluorescence staining further confirmed the upregulation of E-cadherin and downregulation of N-cadherin. (**E**–**G**) Additionally, Western blot analysis revealed lower levels of Vimentin, Snail, and Slug proteins in the Oroxylin A-treated group than in the control group. The experiments were performed three times with consistent results ($^*p < 0.05$ vs. control).

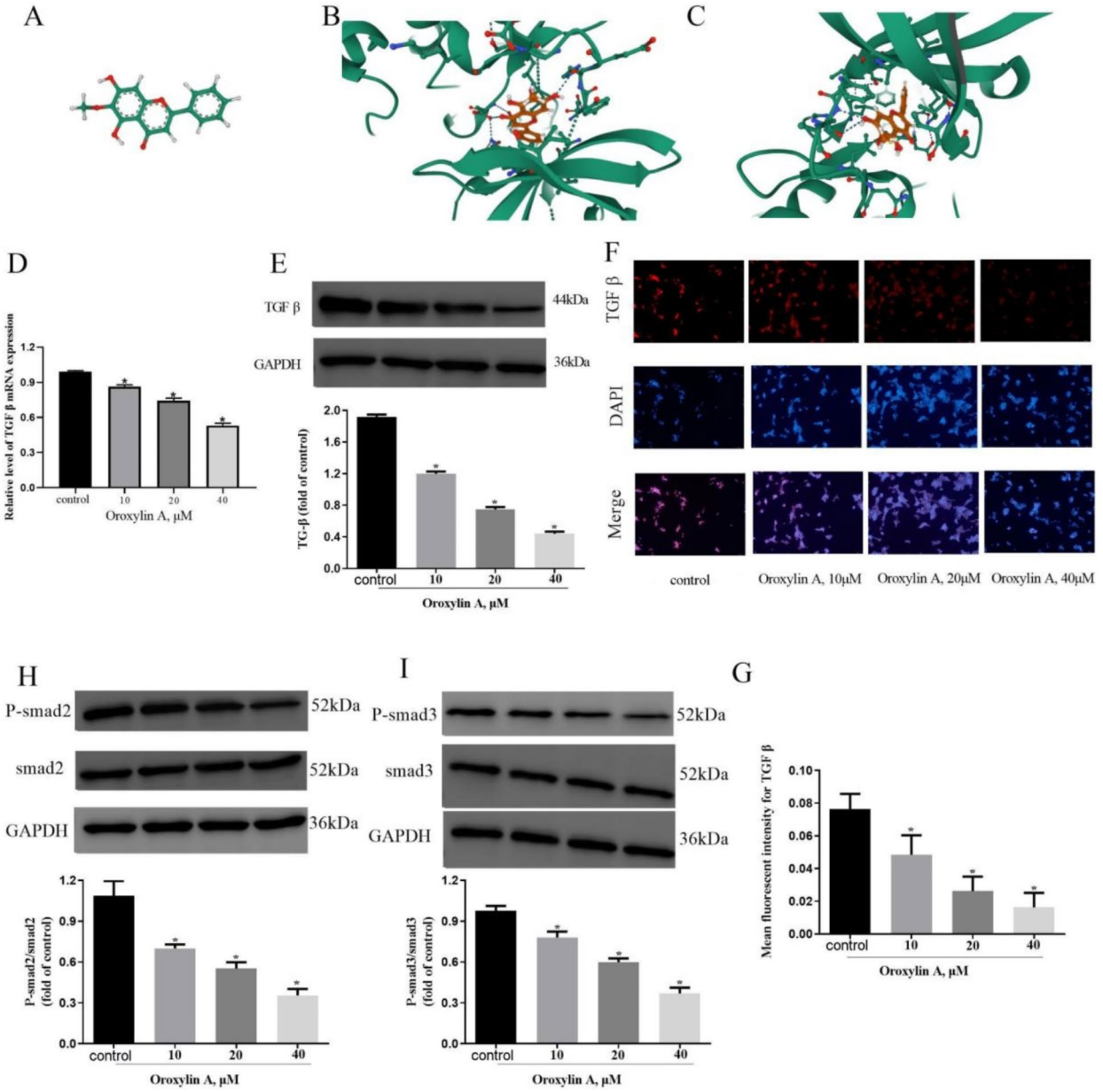

Fig. 7. Target prediction underlying Oroxylin A inhibition of EMT via the molecular docking method. (**A**) 3D structure of Oroxylin A. (**B**) TGF-βI receptors bound to Oroxylin A. (**C**) TGF-βII receptors bound to Oroxylin A. (**D**) RT-PCR experiments showing that Oroxylin A decreased the expression of TGF-β mRNA. (**E**,**H**,**I**) Western blot analysis was performed to investigate the impact of Oroxylin A on the protein expression levels of TGFβ, p-smd2, smad2, p-smad3, and smad3 in HCT116 cells. (**F**,**G**) Immunofluorescence staining revealed a decrease in TGF-β expression. The symbol "*" denotes a significant difference compared with the control group ($P < 0.05$), with $n = 3$ replicates.

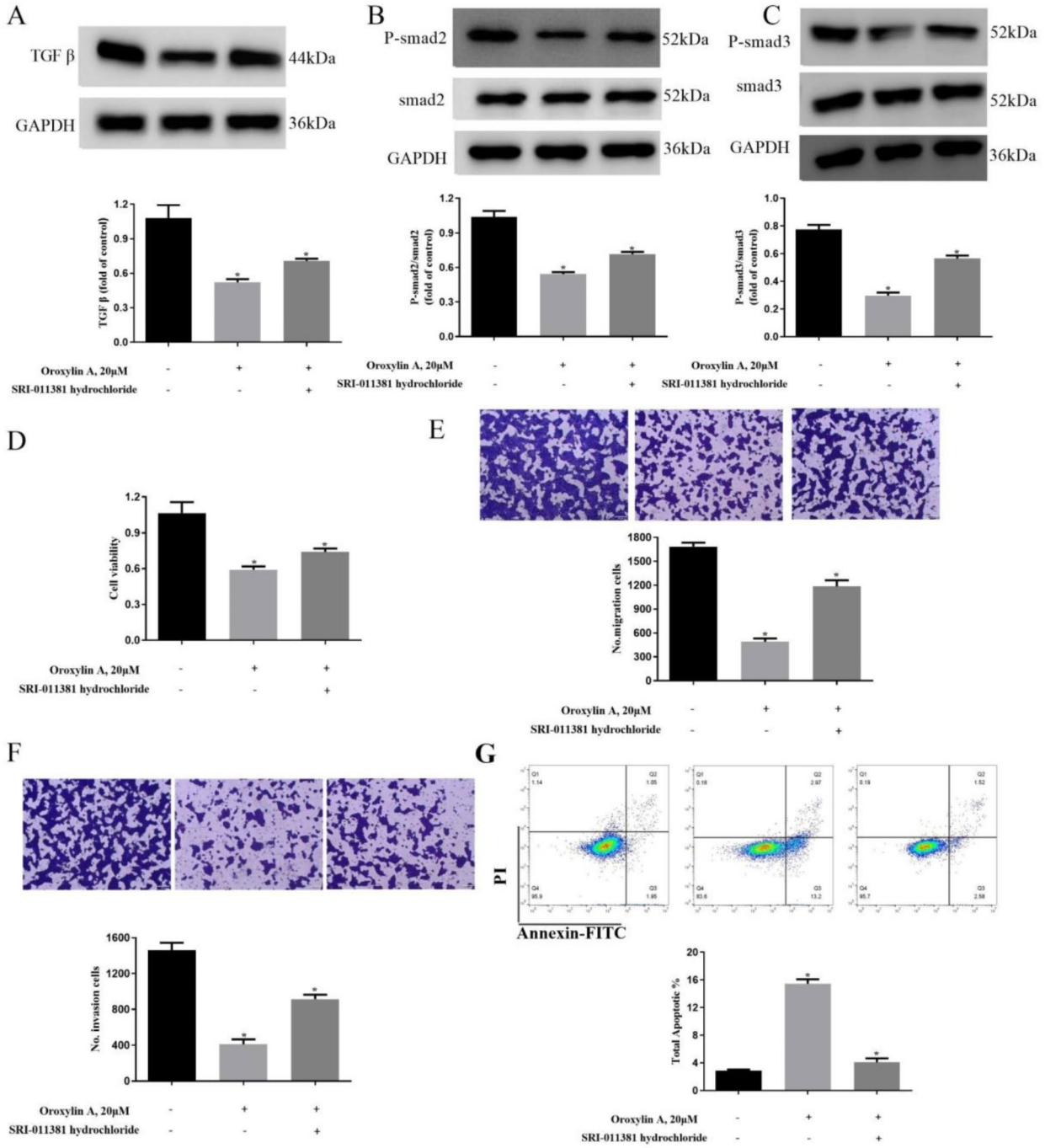

Fig. 8. TGFβ overexpression attenuates the effect of Oroxylin A on human colorectal cancer cells. (**A**–**C**) Western blot analysis revealed a significant increase in the levels of TGFβ, p-smd2/smd2 and p-smad3/smad3 upon treatment with SRI-011381 hydrochloride. (**D**–**G**) Overexpression of TGFβ weakened the inhibitory effect of Oroxylin A on the proliferation, migration and invasion of human colorectal cancer cells, as well as the promoting effect on apoptosis. The symbol "*" denotes statistical significance compared with the control group ($P < 0.05$), with $n = 3$ replicates.

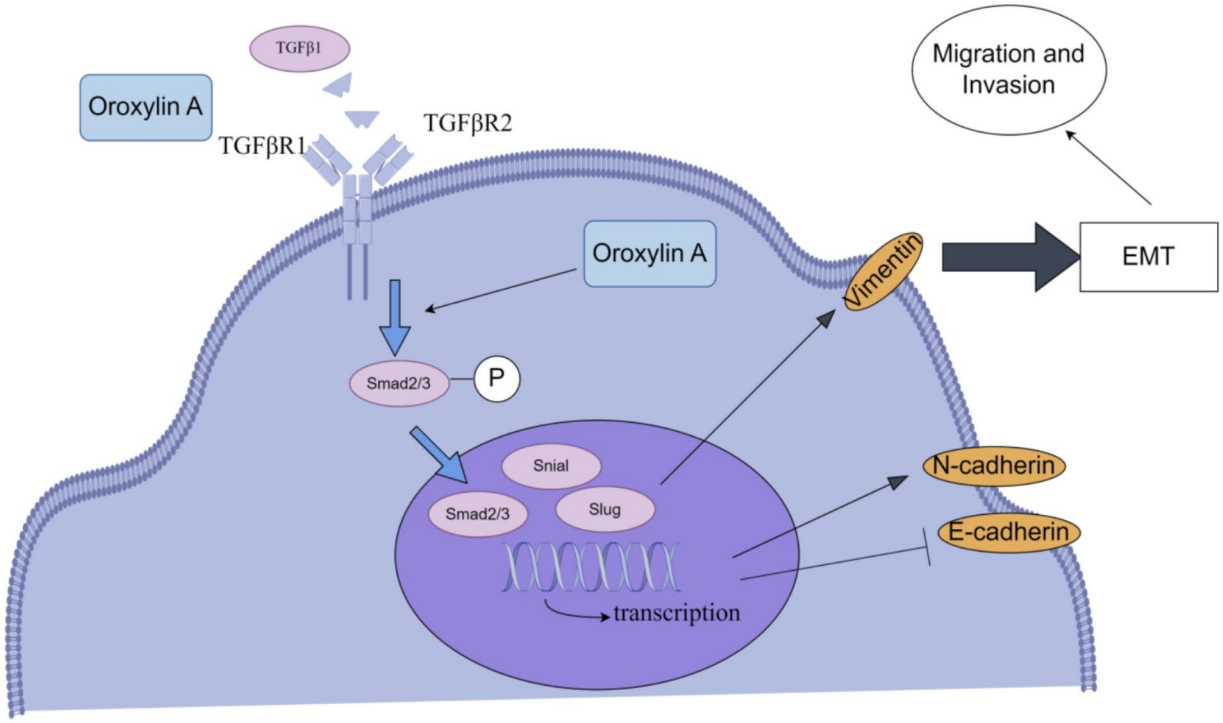

Fig. 9. A schematic representation showed the effect of Oroxylin A on EMT in tumor cells. TGF-β binds to a tetrameric complex of TβRI and TβRII on cell membrane, which consequently phosphorylates Smad2 and Smad3 proteins and activates expression of EMT-inducing transcription factors. Oroxylin A strongly suppresses TGF-β-induced phosphorylation of Smad-2 and -3 and thereby inhibits the downstream EMT program by upregulating the expression of E-cadherin, a marker associated with epithelial cells, while downregulating the levels of N-cadherin, Snail, Vimentin, and slug, which are markers associated with mesenchymal cells.

Data availability

All relevant data are within the paper and its supplementary information files.

Received: 31 May 2024; Accepted: 4 October 2024
Published online: 15 October 2024

References

1. Shin, A. E., Giancotti, F. G. & Rustgi, A. K. Metastatic colorectal cancer: mechanisms and emerging therapeutics. *Trends Pharmacol. Sci.* **44** (4), 222–236 (2023).
2. Araghi, M. et al. Global trends in colorectal cancer mortality: projections to the year 2035. *Int. J. Cancer*. **144** (12), 2992–3000 (2019).
3. Rumpold, H. et al. Prediction of mortality in metastatic colorectal cancer in a real-life population: a multicenter explorative analysis. *BMC Cancer*. **20** (1), 1149 (2020).
4. Cui, J. et al. Regulation of EMT by KLF4 in gastrointestinal cancer. *Curr. Cancer Drug Targets*. **13** (9), 986–995 (2013).
5. Paul, C. D., Mistriotis, P. & Konstantopoulos, K. Cancer cell motility: lessons from migration in confined spaces. *Nat. Rev. Cancer*. **17** (2), 131–140 (2017).
6. Kano, Y., Suenaga, M. & Uetake, H. Strategic insight into the combination therapies for metastatic colorectal cancer. *Curr. Oncol.* **30** (7), 6546–6558 (2023).
7. Lee, G. Y., Lee, J. S., Son, C. G. & Lee, N. H. Combating drug resistance in colorectal cancer using herbal medicines. *Chin. J. Integr. Med.* **27** (7), 551–560 (2021).
8. Cepero, A. et al. Antibody-functionalized nanoformulations for targeted therapy of colorectal cancer: a systematic review. *Int. J. Nanomed.* **17**, 5065–5080 (2022).
9. Henamayee, S. et al. Therapeutic emergence of rhein as a potential anticancer drug: a review of its molecular targets and anticancer properties. *Molecules*. **25** (10), 2278 (2020).
10. Liu, D. M. et al. A new abietane diterpenoid from Ajuga Ovalifolia var. Calantha induces human lung epithelial A549 cell apoptosis by inhibiting SHP2. *Fitoterapia*. **141**, 104484 (2020).
11. Zhang, X. Y. et al. The positive role of traditional Chinese medicine as an adjunctive therapy for cancer. *Biosci. Trends*. **15** (5), 283–298 (2021).

12. Wei, L. et al. Oroxylin A inhibits glycolysis-dependent proliferation of human breast cancer via promoting SIRT3-mediated SOD2 transcription and HIF1α destabilization. *Cell. Death Dis.* **6** (4), e1714 (2015).
13. Jadeja, R. N. et al. Naturally occurring Nrf2 activators: potential in treatment of Liver Injury. *Oxid. Med. Cell. Longev.* **2016**, 3453926 (2016).
14. Lu, L., Guo, Q. L. & Zhao, L. Overview of Oroxylin A: a promising flavonoid compound. *Phytother. Res.* **30** (11), 1765–1774 (2016).
15. Cao, Y. et al. Oroxylin A suppresses ACTN1 expression to inactivate cancer-associated fibroblasts and restrain breast cancer metastasis. *Pharmacol. Res.* **159**, 104981 (2020).
16. Wei, L. et al. Oroxylin A inhibits invasion and migration through suppressing ERK/GSK-3β signaling in snail-expressing non-small-cell lung cancer cells. *Mol. Carcinog.* **55** (12), 2121–2134 (2016).
17. Huo, T. X. et al. Oroxylin A inhibits the migration of hepatocellular carcinoma cells by inducing NAG-1 expression. *Acta Pharmacol. Sin.* **43** (3), 724–734 (2022).
18. Xu, J., Lamouille, S. & Derynck, R. TGF-beta-induced epithelial to mesenchymal transition. *Cell. Res.* **19** (2), 156–172 (2009).
19. Wu, Q. et al. Astrocytic YAP protects the optic nerve and retina in an experimental autoimmune encephalomyelitis model through TGF-β signaling. *Theranostics*. **11** (17), 8480–8499 (2021).
20. Wang, Y. Q. et al. Cancer incidence and mortality in Zhejiang Province, Southeast China, 2016: a population-based study. *Chin. Med. J. (Engl)*. **134** (16), 1959–1966 (2021).
21. Li, Y. et al. Downregulation of MEIS1 mediated by ELFN1-AS1/EZH2/DNMT3a axis promotes tumorigenesis and oxaliplatin resistance in colorectal cancer. *Signal. Transduct. Target. Ther.* **7** (1), 87 (2022).
22. Lu, L., Guo, Q. L. & Zhao, L. Overview of oroxylin A: a promising flavonoid compound. *Phytother. Res.* **30**, 1765–1774 (2016).
23. Shen, L. et al. Clinical utility of contrast-enhanced ultrasonography in the diagnosis of benign and malignant small renal masses among Asian population. *Cancer Med.* **8** (18), 7532–7541 (2019).
24. Polyak, K. & Weinberg, R. A. Transitions between epithelial and mesenchymal states: acquisition of malignant and stem cell traits. *Nat. Rev. Cancer*. **9**, 265–273 (2009).
25. Thiery, J. P. & Sleeman, J. P. Complex networks orchestrate epithelial–mesenchymal transitions. *Nat. Rev. Mol. Cell. Biol.* **7**, 131–142 (2006).
26. Derynck, R., Turley, S. J. & Akhurst, R. J. TGFbeta biology in cancer progression and immunotherapy. *Nat. Rev. Clin. Oncol.* **18** (1), 9–34 (2021).
27. Xu, J., Lamouille, S. & Derynck, R. TGF-beta-induced epithelial to mesenchymal transition. *Cell. Res.* **19**, 156–172 (2009).
28. Deckers, M. et al. The tumor suppressor Smad4 is required for transforming growth factor beta-induced epithelial to mesenchymal transition and bone metastasis of breast cancer cells. *Cancer Res.* **66** (4), 2202–2209 (2006).

Acknowledgements

This work was supported by the National Natural Science Foundation of China (No.82202063), the Jiangsu Pharmaceutical Association-HengRui Hospital Pharmacy Fund (No.H202047), the Nantong First People's Hospital High-level Science and Technology Project Cultivation Fund (No.YPYJJZD007), the Fund of Nantong University (No.2022JZ005, 2022JY004) and the Fund of Drug Policy and Pharmaceutical Care of Nantong City (No.2023NTPA05). The funders had no role in the study design, data collection and analysis, decision to publish, or preparation of the manuscript.

Author contributions

J.-P.C.: analyzing data with the support of the corresponding author; L.-X.Z., Y.Y. and X.-S.L.: software and validation; P.-F.F. and R.-K.H.: conceptualization, data curation, and writing-original draft preparation.

Declarations

Competing interests

The authors declare no competing interests.

Additional information

Supplementary Information The online version contains supplementary material available at https://doi.org/10.1038/s41598-024-75457-3.

Correspondence and requests for materials should be addressed to R.-K.H. or P.-F.F.